NA61/SHINE RESULTS ON SEARCH FOR CRITICAL POINT*

Nikolaos Davis

for the NA61/Shine Collaboration

H. Niewodniczański Institute of Nuclear Physics Polish Academy of Sciences
Radzikowskiego 152, 31-342 Kraków, Poland

Received 9 April 2026, accepted 16 October 2026,
published online 23 October 2026

The NA61/SHINE experiment at the CERN SPS is a multipurpose fixed-target spectrometer for charged and neutral hadron measurements. Its research program is multi-faceted, including, among other goals, the study of strong interactions. One major goal of its strong interaction program is to determine the existence and pinpoint the location of the QCD critical point, an object of both experimental and theoretical studies. This contribution will summarize the current status of NA61/SHINE critical point searches in nucleus–nucleus collisions, in the collision-energy range $\sqrt{s_{NN}}$ = 5–17 GeV. The review includes studies of fluctuations of net-electric charge, femtoscopy analysis of π–π pairs, as well as intermittency of protons and negatively charged hadrons. No clear indication of the critical point has been observed so far. Finally, we report on the development of novel methods aimed at solving the long-standing problem of bin-by-bin correlations in experimental intermittency analysis, and for a more accurate handling of systematics and uncertainties.

DOI:10.5506/APhysPolBSupp.19.5-A18

1. Introduction

NA61/SHINE [1] is the second largest fixed-target experiment at CERN. As a direct, upgraded continuation of its predecessor NA49, the detector offers a nearly continuous experimental data flow for three decades. Its research program includes strong-interaction physics as well as measurements for neutrino (J-PARC, Fermilab) and cosmic-ray studies (such as the Pierre Auger Observatory, Telescope Array, and IceTop). In this paper, only a selected set of most recent results related to the NA61/SHINE critical point search program will be addressed.

* Presented at the 32nd Cracow Epiphany Conference on the Recent Results from Heavy Ion Physics, Kraków, Poland, 12–16 January, 2026.

A key question in the study of non-perturbative QCD is to determine the structure of the QCD phase diagram, that is, the location and type of phase-transition boundaries between the various states of strongly interacting matter, as a function of temperature T and baryochemical potential μ_B (or nuclear density, n_B). Evidence from lattice QCD and effective models indicates a smooth cross-over between hadronic matter and quark–gluon plasma at high T and low μ_B, and a first-order transition at low T and high μ_B, ending at a critical point (CP), in the vicinity of which a second-order transition is widely expected to occur [2–4].

In the vicinity of the CP, enhanced, non-monotonic fluctuations of various observables [5], as well as scale-invariant (power-law) particle correlations [6–8], are expected to occur (Fig. 1 (left)). Correlations in configuration space are projected to momentum space via quantum statistics and collective flow, where they can be observed by collision experiments. In order to do so, one must perform a carefully stepped scan in parameters that can be controlled experimentally, such as collision energy, nuclear mass number, centrality, and others. By varying such parameters, the freeze-out conditions of the colliding systems in (T, μ_B) vary accordingly [9]. NA61/SHINE has completed a two-dimensional scan in collision energy ($\sqrt{s_{NN}}$ = 5–17 GeV) and system size (p+p, p+Pb, Be+Be, O+O, Ar+Sc, Xe+La, Pb+Pb), see Fig. 1 (right); it is therefore in a unique position to pursue the search for critical point signatures in nuclear collisions.

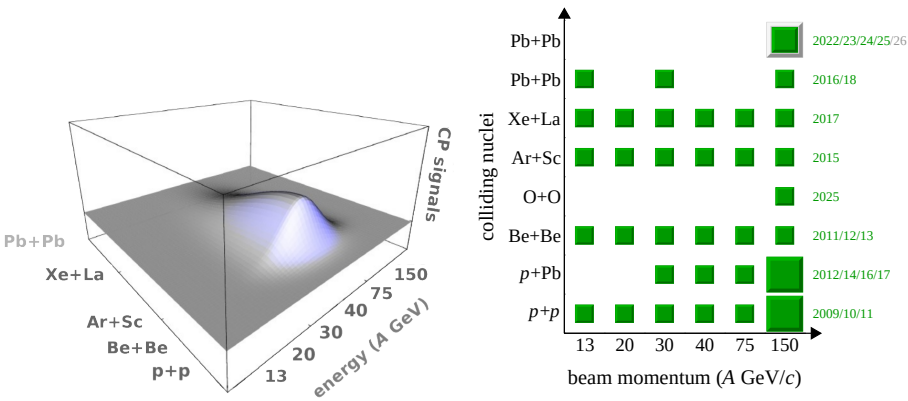


Fig. 1. Left: Schematic representation of "hill of fluctuations" expected around the CP. Right: Status of NA61/SHINE scan in collision energy and system size.

2. Net-electric charge fluctuations

Fluctuations of conserved charges (electric, strangeness or baryon number) are of particular interest in the NA61/SHINE energy-system size scan [10].

To compare fluctuations in systems of different sizes, one should use quantities insensitive to system volume, *i.e.* intensive quantities. They are constructed by division of cumulants κ_i [11, 12] of the measured multiplicity distribution (up to fourth order), where i is the order of the cumulant. In the case of net-charge, cumulant ratios are defined as $\kappa_2[h^+ - h^-]/(\kappa_1[h^+] + \kappa_1[h^-])$, $\kappa_3[h^+ - h^-]/\kappa_1[h^+ - h^-]$, and $\kappa_4[h^+ - h^-]/\kappa_2[h^+ - h^-]$, where $h^{+(-)}$ stands for positively (negatively) charged hadrons.

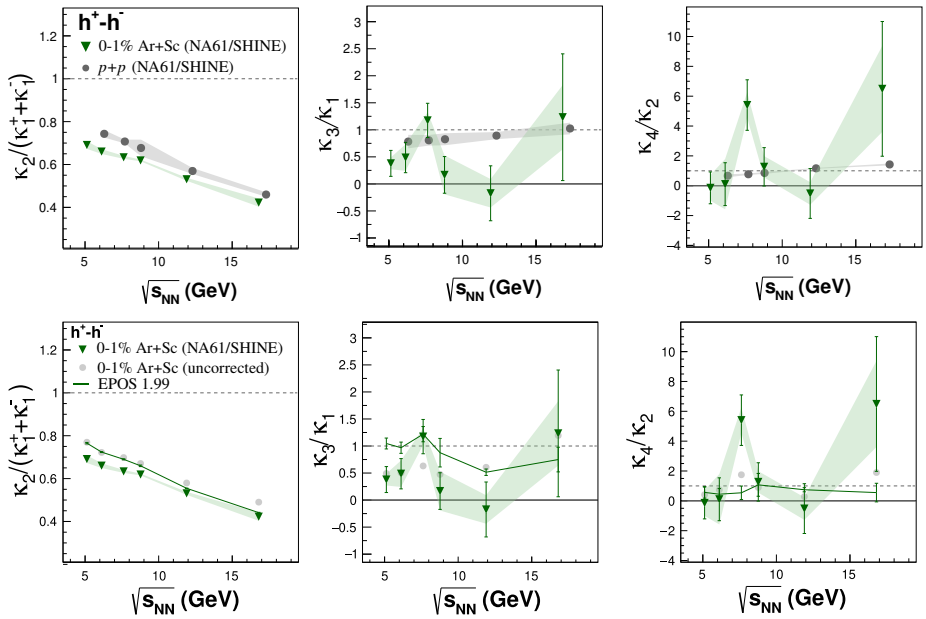


Fig. 2. Top row: The energy dependence of $\kappa_2/(\kappa_1^+ + \kappa_1^-)$ (left), κ_3/κ_1 (middle), and κ_4/κ_2 (right) of net charge in the 1% most central ^{40}Ar+^{45}Sc (triangles) and inelastic p+p NA61/SHINE interactions (gray circles). Bottom row: The same ratios of cumulants as in the top row for ^{40}Ar+^{45}Sc interactions (color triangles) compared with Epos1.99 model predictions (solid color lines). The color triangles correspond to quantities obtained from corrected distributions, while the gray circles correspond to those obtained from the uncorrected distributions (statistical uncertainties are not indicated). The error bars correspond to statistical uncertainties via bootstrap, while the color bands correspond to systematic uncertainties. The dashed line at unity corresponds to the reference value of the Skellam distribution. The solid line at zero corresponds to the case with no fluctuations in the system. Figure adapted from Ref. [12].

Figure 2 shows the system size and energy dependence of second-, third-, and fourth-order cumulant ratios of net-electric charge in p+p and central Ar+Sc interactions [12] (top row), in comparison to the Epos1.99 model predictions (bottom row). Epos1.99 [13] reproduces the magnitude of the signal observed in the data, with the largest deviations occurring at mid-SPS energies. There is a hint of non-monotonic behavior in κ_3/κ_1 and κ_4/κ_2 for central Ar+Sc at mid-SPS energies; however, statistical uncertainties are large. So far, no significant non-monotonic signal has been observed. More detailed studies are needed.

3. Femtoscopy analysis

The study of Bose–Einstein correlations (femtoscopy) in pairs of identical bosons (*e.g.* pions) produced in an ion collision can reveal the space-time structure of the hadron emitting source [14]. In particular, for small to intermediate systems, we compare measurements with source calculations based on Lévy-distributed sources [14] to explore the pair transverse-mass dependence of the Lévy source parameters. The Lévy exponent α is of particular significance, as it characterizes the shape of the source and is sensitive to the system freezing out in the vicinity of the CP.

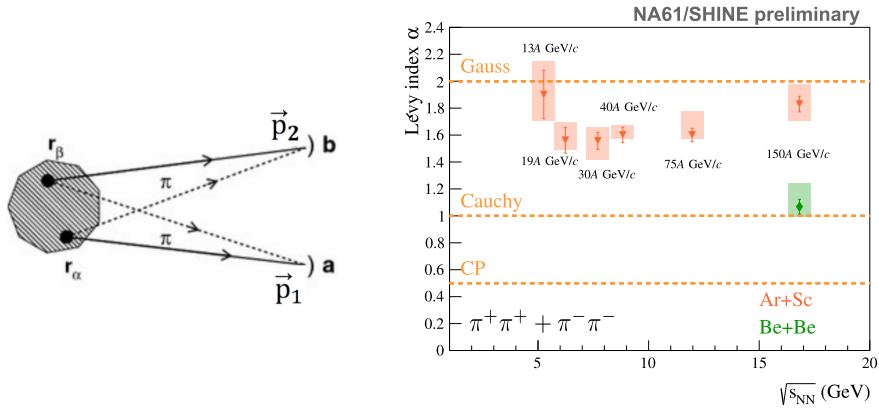


Fig. 3. Left: Schematic representation of a correlated pair of pions emitted from a source. Right: Values of α obtained by fitting the pion pair correlation function, Eq. (1), for pions produced in 0–20% central Be+Be at 150A GeV/c and 0–10% central Ar+Sc collisions at all available energies as a function of $\sqrt{s_{NN}}$. Special cases corresponding to a Gaussian ($\alpha = 2$) or a Cauchy ($\alpha = 1$) source are shown, as well as $\alpha = 0.5$, which corresponds to the critical point [14]. Boxes denote systematic uncertainties, bars represent statistical uncertainties. Figure from Ref [15].

The femtoscopic correlation function fit to the data takes the form

$$C(q) = 1 + \lambda \, \mathrm{e}^{-(qR)^{\alpha}} , \tag{1}$$

where $q = |\boldsymbol{p}_1 - \boldsymbol{p}_2|$ is the momentum difference between bosons in the pair (Fig. 3 (left)), R is the Lévy scale parameter, λ is the correlation strength, and α is the Lévy exponent (index) which is a shape parameter of the distribution (for $\alpha = 2$, we get a Gaussian distribution).

Figure 3 (right) shows the Lévy index α values fitted to $\pi^+\pi^+$ and $\pi^-\pi^-$ pairs produced at different SPS collision energies for Be+Be and Ar+Sc collisions observed by the NA61/SHINE experiment. The recent Ar+Sc results are close to Gaussian, and far from the CP predicted value. No indication of the critical point is observed at any of the investigated energies.

4. Intermittency analysis

A characteristic feature of a second-order phase transition is the divergence of the correlation length of the physical system, leading to a scale-invariant system with long-range correlations. The density–density correlation function of the phase-transition order parameter (for example, the chiral σ-condensate or the net-baryon density n_B [16]) assumes a power-law form, with critical exponents determined by the 3D Ising universality class [6–8]. Observables tailored for probing such power-law behavior are the scaled factorial moments (SFMs) $F_r(M)$ in transverse momentum space

$$F_r(M) \equiv \left\langle \frac{1}{M^2} \sum_{m=1}^{M^2} n_m(n_m - 1) \ldots (n_m - r + 1) \right\rangle \Bigg/ \left\langle \frac{1}{M^2} \sum_{m=1}^{M^2} n_m \right\rangle^{r} , \tag{2}$$

where n_m is the number of particles in a transverse momentum (p_x, p_y) bin in an event, M^2 is the total number of 2D bins, and $\langle \ldots \rangle$ denotes averaging over events. Intermittency is defined as a power-law scaling of $F_r(M)$ with the number of bins, or equivalently bin size: $F_r(M) \sim (M^2)^{\phi_r}$, with ϕ_r being the r^{th}-order intermittency index [8, 17]. For protons[1] and $r = 2$, $\phi_2 = 5/6$ is expected [8]. When probing intermittent behavior, baseline correlations have to be subtracted; this can be done either through the cumulative variable transform, imposing a uniform 1-particle (p_x, p_y) distribution [18–20], or by subtracting mixed event moments from those of data [21]; the resulting subtracted scaled factorial moments carrying the possible critical signal are denoted by $\Delta F_r(M)$ or $\Delta F_r(M)_c$ for cumulative.

[1] Protons substitute for net baryons [16], an approximation that is valid when antiprotons are much fewer than protons in events.

Figure 4 (left) shows the behavior of proton multiplicity moments $\Delta F_2(M)_c$ for a number of NA61/SHINE Ar+Sc collision datasets in the momentum range 13A–150A GeV/c ($\sqrt{s_{NN}}$ = 5–17 GeV). The number of transverse-momentum-space subdivisions (bins) ranges from $1^2 \leq M^2 \leq 150^2$, within a window $-1.5 \leq p_{x,y} \leq 1.5$ GeV/c at mid-rapidity. No intermittency signal indicative of the CP is observed.

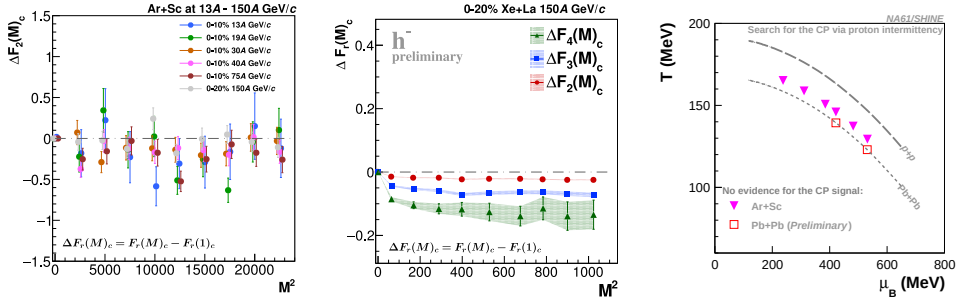


Fig. 4. Left: Results on the proton multiplicity second-order SFMs $\Delta F_2(M)_c$ for NA61/SHINE Ar+Sc collisions in the momentum range 13A–150A GeV/c ($\sqrt{s_{NN}}$ = 5–17 GeV) [19, 20]. Middle: second- through fourth-order SFMs for NA61/SHINE negatively charged hadrons in Xe+La collisions at 150A GeV/c ($\sqrt{s_{NN}}$ = 16.8 GeV) [22]; cumulative variables [18] and independent bins are used. Right: Status of NA61/SHINE CP search via proton intermittency [20]. Points indicate freeze-out conditions of respective reactions in (T, μ_B). Figure from Ref. [20].

NA61/SHINE also looked into negatively charged hadrons (h^-) intermittency in Xe+La collisions at 150A GeV/c ($\sqrt{s_{NN}}$ = 16.8 GeV), as a check of the published STAR Collaboration intermittency results for all charged hadrons in Au+Au collisions [23]. Figure 4 (middle) shows NA61/SHINE h^- results for r = 2–4 SFMs. When a cumulative transform is applied to the momenta in order to remove baseline/spurious effects, no intermittency effect remains. The effect similarly vanishes when a short-range correlation cut is applied, suggesting HBT-like correlations are at the origin of the observed effect [22].

Figure 4 (right) summarizes NA61/SHINE system size and energy proton intermittency scan, showing the estimated freeze-out conditions for the analyzed systems; so far, no significant intermittency signal is observed.

The above presented NA61/SHINE intermittency results utilize independent bins in order to avoid M-bin correlations, which invalidate fitting and comparison with models. This method has the drawback of reducing event statistics per bin, thus significantly inflating uncertainties. An alternative approach has been developed to handle bin correlations [25], based on the statistical tool of Principal Component Analysis (PCA). Figure 5 illustrates

how PCA works: a set of original moments generated via the Critical Monte Carlo (CMC) simulation [8, 25] (left) are transformed into statistically independent linear combinations of the original M-bins, called the principal components (PCs) (middle). A power-law candidate model (black points), $\Delta F_2^{\text{model}}(M) \equiv 10^{\alpha_0} \left(\frac{M^2}{10^4}\right)^{\phi_2}$ is transformed in the same way, and its residuals are compared to the data bootstrap variance in the PCs. The result is a likelihood value for the model, which can be collected into a likelihood distribution of model parameters (right). This allows for the reliable extraction of ϕ_2 and other parameter confidence intervals from correlated data, making use of the full event statistics. We expect this method to permit more reliable studies of intermittency phenomena, in NA61/SHINE as well as other high-energy physics experiments.

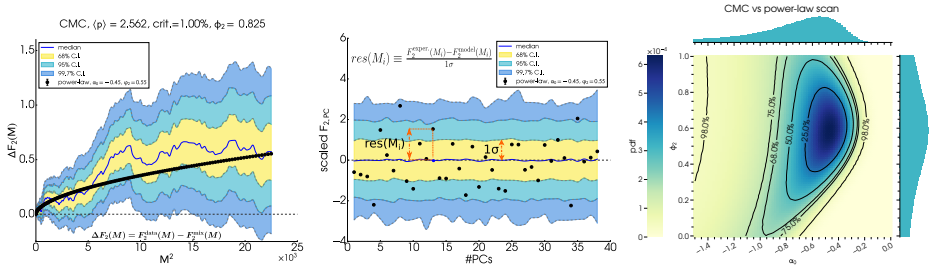


Fig. 5. Left: Correlated proton $\Delta F_2(M)$ for $\sim$ 8K bootstrap samples [24] of a synthetic CMC data set (colored bands) corresponding to $\sim$ 400K Ar+Sc-like collisions with 1% critical protons. Black points represent a power-law model fit, with parameters (α_0, ϕ_2). Middle: $\Delta F_2(M)$ for the same CMC data set, transformed to the PC coordinates. Right: Normalized likelihood distribution for a grid of parametrized power-law models against the same CMC data set. Figures adapted from Ref. [25].

5. Summary

In this work, we have provided an overview of the NA61/SHINE critical point search program, including net-charge fluctuations, femtoscopy analysis, and intermittency analyses on both protons and negatively charged hadrons for a variety of system sizes and SPS collision energies. Findings from NA61/SHINE give no clear indication of the critical point so far; however, they point at the crucial importance of a proper understanding of non-critical (baseline) effects in the CP search.

We report a new development in intermittency analysis, which effectively solves the long-standing bin-by-bin correlation problem [25]; this allows the use of full statistics with correlated bins and reliable model scans to locate the best-fitting models to the data. Event statistics plays a crucial role, as

intermittency analysis is particularly data-hungry. Nevertheless, it is within the capabilities of the upgraded NA61/SHINE detector to provide sufficient data for such analyses.

The present work was supported by the Polish Ministry of Science and Higher Education (2025/WK/05).

REFERENCES

[1] NA61/SHINE Collaboration (N. Abgrall *et al.*), *J. Instrum.* **9**, P06005 (2014), arXiv:1401.4699 [physics.ins-det].

[2] S. Borsányi *et al.*, *Phys. Rev. D* **111**, 014506 (2025).

[3] B.J. Schaefer, M. Wagner, *Prog. Part. Nucl. Phys.* **62**, 381 (2009).

[4] J.I. Kapusta, S. Wan, *Phys. Rev. C* **113**, 035207 (2026).

[5] M. Gazdzicki, P. Seyboth, *Acta Phys. Pol. B* **47**, 1201 (2016), arXiv:1506.08141 [nucl-ex].

[6] N.G. Antoniou *et al.*, *Nucl. Phys. A* **693**, 799 (2001), arXiv:hep-ph/0012164.

[7] N.G. Antoniou, Y.F. Contoyiannis, F.K. Diakonos, G. Mavromanolakis, *Nucl. Phys. A* **761**, 149 (2005), arXiv:hep-ph/0505185.

[8] N.G. Antoniou, F.K. Diakonos, A.S. Kapoyannis, K.S. Kousouris, *Phys. Rev. Lett.* **97**, 032002 (2006), arXiv:hep-ph/0602051.

[9] F. Becattini, J. Manninen, M. Gaździcki, *Phys. Rev. C* **73**, 044905 (2006), arXiv:hep-ph/0511092.

[10] NA61/SHINE Collaboration (H. Adhikary *et al.*), Tech. Rep. CERN-SPSC-2022-034, SPSC-SR-319, CERN, Geneva, 2022.

[11] M. Asakawa, M. Kitazawa, *Prog. Part. Nucl. Phys.* **90**, 299 (2016).

[12] NA61/SHINE Collaboration (H. Adhikary *et al.*), *Eur. Phys. J. C* **85**, 918 (2025), arXiv:2503.22484 [nucl-ex].

[13] K. Werner, F.-M. Liu, T. Pierog, *Phys. Rev. C* **74**, 044902 (2006), arXiv:hep-ph/0506232.

[14] T. Csörgő, S. Hegyi, T. Novak, W.A. Zajc, *AIP Conf. Proc.* **828**, 525 (2006), arXiv:nucl-th/0512060.

[15] NA61/SHINE Collaboration (B. Porfy), *PoS* **(ICHEP2024)**, 603 (2025), arXiv:2410.13975 [nucl-ex].

[16] Y. Hatta, M.A. Stephanov, *Phys. Rev. Lett.* **91**, 102003 (2003); *Erratum ibid.* **91**, 129901 (2003), arXiv:hep-ph/0302002.

[17] A. Bialas, R.B. Peschanski, *Nucl. Phys. B* **273**, 703 (1986).

[18] A. Bialas, M. Gazdzicki, *Phys. Lett. B* **252**, 483 (1990).

[19] NA61/SHINE Collaboration (H. Adhikary *et al.*), *Eur. Phys. J. C* **83**, 881 (2023), arXiv:2305.07557 [nucl-ex].

[20] NA61/SHINE Collaboration (H. Adhikary *et al.*), *Eur. Phys. J. C* **84**, 741 (2024), arXiv:2401.03445 [nucl-ex].

[21] NA49 Collaboration (T. Anticic *et al.*), *Eur. Phys. J. C* **75**, 587 (2015), arXiv:1208.5292 [nucl-ex].

[22] NA61/SHINE Collaboration (V.Z.R. Ortiz), *Ukr. J. Phys.* **69**, 858 (2024).

[23] STAR Collaboration (M. Abdulhamid *et al.*), *Phys. Lett. B* **845**, 138165 (2023), arXiv:2301.11062 [nucl-ex].

[24] W.J. Metzger, «Estimating the Uncertainties of Factorial Moments», 2004, HEN-455, unpublished.

[25] N. Davis, *Phys. Lett. B* **868**, 139697 (2025), arXiv:2409.14185 [physics.data-an].